Current Zoology, 2022, **XX**, 1–10
https://doi.org/10.1093/cz/zoac042
Advance access publication 25 May 2022
Original Article

Declining metabolic scaling parallels an ontogenetic change from elongate to deep-bodied shapes in juvenile Brown trout

Jorge-Rubén Sánchez-González[a,c], and Alfredo G. Nicieza[a,b,*]

[a]Department of Organisms and Systems Biology, University of Oviedo, 33006 Oviedo, Spain
[b]Biodiversity Research Institute (IMIB), University of Oviedo-Principality of Asturias-CSIC, 33600 Mieres, Spain
[c]Department of Animal Science-Wildlife Section, University of Lleida, 25006 Lleida, Spain

[*]Address correspondence to Alfredo G. Nicieza. E-mail: agnic@uniovi.es
Handling editor: Zhi-Yun Jia

Abstract

Body shape and metabolic rate can be important determinants of animal performance, yet often their effects on influential traits are evaluated in a non-integrated way. This creates an important gap because the integration between shape and metabolism may be crucial to evaluate metabolic scaling theories. Here, we measured standard metabolic rate in 1- and 2-years old juvenile brown trout *Salmo trutta*, and used a geometric morphometrics approach to extricate the effects of ontogeny and size on the link between shape and metabolic scaling. We evidenced near-isometric ontogenetic scaling of metabolic rate with size, but also a biphasic pattern driven by a significant change in metabolic scaling, from positive to negative allometry. Moreover, the change in metabolic allometry parallels an ontogenetic change from elongate to deep-bodied shapes. This is consistent with the dynamic energy budget (DEB) and surface area (SA) theories, but not with the resource transport network theory which predicts increasing allometric exponents for trends towards more robust, three-dimensional bodies. In addition, we found a relationship between body shape and size independent metabolic rate, with a positive correlation between robustness and metabolic rate, which fits well within the view of Pace-of-Life Syndromes (POLS). Finally, our results align with previous studies that question the universality of metabolic scaling exponents and propose other mechanistic models explaining the diversity of metabolic scaling relationships or emphasizing the potential contribution of ecological factors.

Key words: biphasic allometric scaling, metabolic rate, ontogenetic allometry, shape, surface-area, trout.

Maintenance metabolic rate (Mathot and Dingemanse 2015) is a fundamental trait for animal survival and performance under periods of fasting and nutritional stress. In ectotherms it is described by standard metabolic rate (SMR) (Priede 1985), which represents the minimum metabolic rate of non-torpid animals needed to sustain life processes at a given temperature (Naya and Bozinovic 2012). SMR has been positively correlated with growth potential and competitive ability (Metcalfe et al. 1995; Norin et al. 2016; Archer et al. 2021), although it is aerobic scope (i.e., difference between maximal and minimum metabolism) that determines the energy available for performance functions (Van Leeuwen et al. 2011; Biro and Stamps 2010). More specifically, behaviours having consequences for energy gain (e.g. foraging, boldness, dominance) or loss (e.g. locomotor performance) have strong positive correlations with maintenance metabolic rate (Mathot et al. 2019). In turn, low SMRs can be adaptive under conditions of hypoxia (Killen et al. 2016), desiccation and nutritional stress (Hoffmann and Parsons 1989; Djawdan et al. 1997; Matzkin and Markow 2009; Schimpf et al. 2012). There is also evidence for a negative correlation between SMR and growth in the wild (Álvarez and Nicieza 2005; Robertsen et al. 2014; but see Arnold et al. 2021). These opposed scenarios are known as the 'increased intake' or 'performance' hypothesis, and the 'compensation' or 'allocation' hypothesis (Arnold et al. 2021). A third, mixed scenario is given by the 'context dependent' hypothesis: the sign of the relationship between minimum metabolic rates and fitness depends upon the requirements to resource availability ratios (Burton et al. 2011; Careau and Garland 2012; Arnold et al. 2021).

Body shape has important implications for an organism's performance (Wainwright 1994; Rincón et al. 2007). Since shape and metabolic rate are closely intertwined with organisms' size (Kleiber 1947; Gould 1966; Mosimann 1970), an interesting question is whether intra-specific differences in mass- or size-corrected metabolic rate can derive, at least partially, from shape changes. Size, shape and metabolic rate have been identified as predictors of dominance and others traits that can enhance fitness (Swain and Holtby 1989; Holtby et al. 1993; Nicieza and Metcalfe 1999; McCarthy 2000, 2001; Lahti et al. 2002). Physiological, behavioral, and life-historical traits are usually integrated within the concept of pace-of-life syndrome (POLS) (Promislow and Harvey 1990; Ricklefs and Wikelski 2002; Biro and Stamps 2010; Careau et al. 2010, 2011; Réale et al. 2010). Yet, in the context of POLS, empirical studies of relationships between metabolic

Received 18 February 2022; revised 16 May 2022; accepted 17 May 2022

rate and shape are still uncommon, likely due to a narrow definition of POLS (but see Dammhahn et al. 2018; Polverino et al. 2018; Sowersby et al. 2021). This may be paradoxical, because metabolism is a pivotal trait in the POLS context, changes in shape can affect both metabolism and its scaling with size, metabolism has been associated to body, cell, or colony shape in a variety of organisms (Brown and Lasiewski 1972; McMahon 1973; Davies 1980; Porter and Kearney 2009; Nespolo et al. 2011; White et al. 2011; Banavar et al. 2014; Glazier 2014; Hartikainen et al. 2014; Killen et al. 2016; Lagos et al. 2017; Tan et al. 2019; Rubio-Gracia et al. 2020), and morphology is tightly linked with drivers of performance and behavioural traits (e.g., locomotion, agonistic interactions, or mate choice) (Arnold 1983; Molina-Borja et al. 1998; Perry et al. 2004; Lappin and Husak 2005; Peterson and Husak 2006; Huyghe et al. 2010; Martínez-Cotrina et al. 2014).

In addition, two major theories predict metabolic scaling from the relationships between size, growth and geometric constraints affecting the diffusion and transport of materials: the surface area (SA) theory (Okie 2013), which includes DEB (dynamic energy budget) models (Kooijman 2010; Sousa et al. 2010), and the Resource–Transport Network theory (RTN; also metabolic theory of ecology, MTE) (West et al. 1999; Brown et al. 2004; Savage et al. 2008; Banavar et al. 2010; but see Glazier 2014 for broader scope of metabolic theories). SA theory builds on the idea that resource uptake and waste removal depend on external exchange surfaces (Okie 2013; Hirst et al. 2017), and DEB models specifically focus on the surface area involved in uptake, which, in turn depends on the overall body shape (Kooijman 2010; Kearney and White 2012). In contrast, RTN theory is based on the optimization of resources transport from a central hub through fractal-like networks (West et al. 1997, 1999; Brown et al. 2004; Savage et al. 2008; Banavar et al. 2010), and the POLS concept is a central assumption of this theory (Glazier 2015). Both competing theories highlight the role of shape on metabolism (van der Meer 2006; White et al. 2011; Kearney and White 2012; Hirst et al. 2014, 2017; Glazier et al. 2015), but lead to opposite predictions of how body shape changes over ontogeny will affect the metabolic scaling exponent b; for ontogenetic trends towards less flat/elongated and more robust/three-dimensional shapes, SA theory predicts decreasing b whereas RNT theory predicts increasing b (West et al. 1997; Kearney and White 2012; Hirst et al. 2014, 2017; Glazier et al. 2015).

In fusiform fishes like salmonids, a shift from slender to robust shapes results from allometric growth, although the 'elongated-robust' continuum can be also a component of the phenotypic variation within age-classes (Price et al. 2019). Here, we investigated the relationship between mass- and size-independent SMR and body shape in juvenile brown trout (*Salmo trutta* L.) from two age-classes (8- and 20-mo old) to explore two opposing hypotheses relating shape and basal metabolism at the intraspecific level. In the context of POLS (Promislow et al. 1990; Ricklefs and Wikelski 2002; Biro and Stamps 2010; Careau et al. 2010; Réale et al. 2010; Careau and Garland 2012), metabolic rate is assumed to be a hub for the 'slow–fast' pace of life continuum (Ricklefs and Wikelski 2002; Brown et al. 2004; Careau et al. 2011; Glazier 2015; Auer et al. 2018a; Arnold et al. 2021). Here we were aimed to test two working hypothesis that can be implemented within the wider theoretical frameworks of POLS and surface-area models. First, according to the POLS framework and previous research reporting positive links between SMR, dominance and growth (Metcalfe et al. 1995; McCarthy 2000, 2001; Lahti et al. 2002; Norin et al. 2016; Auer et al. 2018b; see also Mathot et al. 2019), we predicted that deep-bodied fish, which tend to be more aggressive than elongate conspecifics (Swain and Holtby 1989; Warner and Schultz 1992; Holtby et al. 1993; Fruciano et al. 2012), will have higher mass- or size-independent metabolic rates than slender fish (hypothesis I). Second, in the absence of isometric scaling, larger animals should have lower mass- or size-specific resting metabolic rates than smaller ones of the same shape (isomorphs) because of a lower surface-to-mass ratio (Savage et al. 2007; Kooijman 2010). By the same logic, equal 'sized' (i.e., mass or volume) animals having different shapes should differ in mass-specific SMRs (Kooijman 2010; Okie 2013). In teleosts, the skin is permeable to water (Talbot et al. 1982; Styga et al. 2019). In the case of salmonids, the early alevin is relatively impermeable to water and ions, but body surface permeability increases as alevin develops (Talbot et al. 1982). Freshwater fish are hyperosmotic and may spend more than 20–50% of their energy budget on osmoregulation to combat the constant influx of water (Boeuf and Payan 2001). Because the rate of diffusion is proportional to the surface area, a greater surface area may involve higher maintenance costs. Thus, since shape can affect not only metabolic scaling exponents (Kearney and White 2012; Hirst et al. 2014, 2017; Glazier et al. 2015), but also the elevation of the metabolic allometries (Yagi and Oikawa 2014), we anticipate that more elongated fish (with a higher surface area to mass ratio) will have higher mass-specific SMRs than robust fish (hypothesis II).

Materials and Methods

Experimental animals

We used 238 trout aged 0+ (8-mo old) and 88 aged 1+ (20-mo old). The fish were originated from wild adults from river Sella (Asturias, northern Spain), raised in River Espinareu hatchery (Centro Ictiogénico de Infiesto; Principality of Asturias). Each year, 30 males and 30 females were used to produce a pool of several thousands of fertilised eggs by crosses of 3–4 females and 3–4 males. In each cross, the eggs from of all females were pooled and then fertilised with the sperm of all males. Embryos and juveniles were reared at the facilities of the Espinareu River hatchery centre (Centro Ictiogénico de Infiesto, Principado de Asturias) until they were transferred to the laboratory at the University of Oviedo, and and kept in holding tanks at 14 °C, natural photoperiod, and fed ad libitum with commercial salmonid food (Sánchez-González and Nicieza 2017).

Measurement of standard metabolic rate

We measured SMR in a flow-through system by using a thermostatted cell (MC 100, Strathkelvin Instruments Ltd, Glasgow, UK) equipped with a microcathode oxygen electrode (Model 1302, Strathkelvin Instruments Ltd) connected to an oxygen meter (Model 781, Strathkelvin Instruments Ltd). The system consisted of 19 cylindrical chambers (internal dimensions: 26 × 154 mm; volume 81.76 cm^3) immersed in a water bath at 14.8 ± 0.1 °C and supplied with air-saturated water (100% O_2). Prior to measure SMR, fish were unfed for 48 h to arrest food digestion, and then they were acclimatised in the chambers for additional 15–20 h in darkness to ensure that rates of oxygen consumption get into a steady baseline state.

For each individual, SMR was recorded at least twice, with a time interval of 90 min between measurements, in order to ensure that conditions within chambers had reached initial state. SMRs (μg O_2 h^{-1}) were calculated from the difference between outflow oxygen content in a control (empty) chamber and the fish chamber (Cutts et al. 1998, 2002; Álvarez et al. 2006; Cano and Nicieza 2006; Sánchez-González 2015). We adjusted flow rate (mean ± 1*SD*: 15.71 ± 1.39 ml min^{-1}) and trial duration to ensure that consumption rates were not affected by low O_2 levels. Final oxygen saturation in the chambers always remained above 90% (see Cutts et al. 1998, 2002; Álvarez and Nicieza 2005; Álvarez et al. 2006; Cano and Nicieza 2006; Sánchez-González 2015 for full details on the respirometry procedure). There was no consistent pattern or significant difference between the first and second measurements of SMR (mean ± 1*SE*: 599.8 ± 22.2 and 611.9 ± 22.9 μg O_2 h^{-1}, for first and second SMR, respectively; Wilcoxon signed-rank test, $Z = 0.60$, $n = 246$, $P = 0.545$).

Morphometric data and shape analysis

After measuring SMR, all the fish were anaesthetized in a solution of benzocaine (50 mg L^{-1}), measured (fork-length, ± 0.01 mm; the length of a fish from the tip of its nose to the deepest point of the notch in the caudal fin), and weighed (± 0.01 g) with a portable precision balance (Mettler Toledo PL83-S). Fish were placed on their right side in a relaxed position, aligned on a grid board, and checked for linearity of the midline in order to avoid arching effects (Valentin et al. 2008; Sánchez-González and Nicieza 2017). Then, images of their left side were captured with a digital camera; all images were re-scaled to 8 cm width and 300 ppi.

We captured 14 morphometric landmarks (Figure 1) using tpsDig 2.22 (Rohlf 2015a,b). We used a Generalized Procrustes Analysis (GPA; Dryden and Mardia 2016) to superimpose, align, scale and rotate landmark coordinates to a consensus coordinate system using tpsRelw 1.53 (Rohlf 2015a, 2016), and a thin-plate spline analysis to obtain 24 partial warps (22 uniform and 2 non-uniform shape variables (Rohlf 2015a; Rohlf et al. 1996; Nespolo et al. 2011). Thin-plate spline analysis and these partial warps were used to visualize shape changes (Zelditch et al. 2004).

Statistical analyses

We conducted a Principal Component Analysis (PCA) on the variances-covariances matrix (McGarigal et al. 2000; Zelditch et al. 2004) of the 24 shape variables and generated a set of independent shape components. We combined the Kaiser-Guttman criterion, visual inspection of scree graphs and a broken-stick procedure to estimate the number of non-trivial components (Jackson 1993; Peres-Neto et al. 2005). In addition, we conducted a discriminant function analysis (DFA) on the partial warps to explore the morphological divergence between cohorts (Zelditch et al. 2004). A priori probabilities were adjusted from the default according to the proportions of 0+ (0.73) and 1+ individuals (0.27). Cross-validation of the discriminant functions was conducted by random resampling of experimental individuals on subsamples containing 90% of the cases for generating the discriminant functions, and 10% cases to evaluate classification accuracy. The bootstrapping procedure was carried out in a loop of 1000 random samples.

After the exploratory DFA (McGarigal et al. 2000), we conducted a MANOVA of non-trivial components (PC1–PC5) to test whether the differences in shape were statistically significant. To equalize sampling variances, for the general linear models we generated a balanced data set by random sampling of 88 cases from the age-0 group. The visual inspection of residuals did not reveal strong departures from normality, and data met the assumption of equality of variance-covariance matrices (Box $M = 19.29$, $df = 15$, $P = 0.228$). Separate ANOVAs for these relative warps were conducted, controlling the false discovery rate (Benjamini and Hochberg 1995) after detection of significant multivariate effects.

Body mass has an obvious implication for metabolism. However, since body mass and shape are not necessarily independent, some of the influence of body shape on SMR might be removed by removing the effect of body mass. Even though extracting the shape variables from the raw data of landmark coordinates removes size variation per se, the shape data may still contain a component of size-related variation due to the effects of allometry (Klingenberg 2016). Therefore, to examine the relationship between metabolic rate, shape and age, we used two proxies of body size: wet

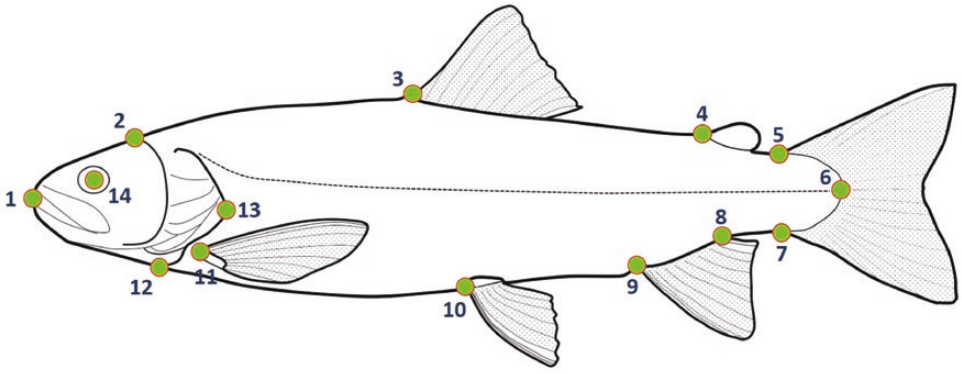

Figure 1. Morphometric landmarks used for the shape analyses of brown trout: (1) Snout tip; (2) posterior supraoccipital notch, (3) anterior insertion of the dorsal fin; (4) anterior insertion of adipose fin; (5) superior and (7) inferior insertions of the caudal fin; (6) posterior body extremity at the junction of lateral line and caudal fin; (8) posterior and (9) anterior insertions of the anal fin; (10) anterior insertion of the pelvic fin; (11) superior insertion of the pectoral fin; (12) insertion of the operculum on the ventral lateral profile; (13) posterior tip of the operculum; (14) centre of the eye. Drawing credit: Jorge-Rubén Sánchez-González.

mass and centroid size (CS). CS is a measure of geometric scale calculated as the square root of the sum of the squared distances from each landmark to the centroid of the configuration (Claude 2008), and the most commonly used measure of size for landmark configurations (Rohlf et al. 1996; Monteiro 1999; Klingenberg 2016; Dryden and Mardia 2016). Body mass and metabolic rate were $\log_{10}$-transformed to meet the assumptions of linearity and homoscedasticity, and to explore the allometric slopes of metabolic rate. We conducted ANCOVAs of log-SMR by age with log-mass (or log-CS). First, we compared the allometric exponents (slopes) of the two age-classes; if the age by size interaction is not significant, an ANCOVA without the interaction term can be used to check for differences in metabolic rate adjusted for size variation. Second, we performed multiple regression of SMR on body size (Cs or mass) and shape variables to further assess the effect of shape change on metabolic rates after taking into account size variation.

Multivariate normality was tested using the '*mvnormtest*' package in R and the Shapiro-Wilk test for multivariate normality (Jarek 2012). Levene and Cochran's *C* tests were used to evaluate the homogeneity of variances, and the Box's *M* test to check the assumption of homogeneity of the dispersion matrices. Statistical analyses were performed using R version 3.6.1 (R Core Team 2019).

Results

Ontogenetic shape allometry

The first three principal components from a PCA on partial warps summarized 49.7% of total variance (64.3% and 82.0% for the first five and nine components, respectively). PC1 (25.8%) reflects a contrast between deep-bodied and elongate forms. Along this elongation axis, individuals with a larger dorsoventral distance and a lower position of the head ("bull" shape) had the higher positive scores (and they were mostly age 1+), whereas more elongated shapes (mostly age 0+) scattered on the negative area (Figure 2). In turn, PC2 (14.3%) reflects disparity in the relative position of the caudal region: fish with a high score on PC2 have a lower relative position of their tail. Discriminant analyses corroborated that juvenile trout can be assigned to their age-class in function of shape: a DFA performed on the partial warps successfully classified 98.15% of the fish to different age groups (Wilks' λ = 0.211, $F_{24,301}$ = 46.88; P < 0.00001). Cross-validation confirmed a high overall rate of correct assignation of 97.0%, with success rates of 100% and 90.9% for classes 0+ and 1+, respectively.

A MANOVA of shape based on the most relevant components (PC1–PC5) confirmed the differences between cohorts (Wilks λ = 0.31, $F_{5,170}$ = 77.28, P < 0.00001). There were no significant differences for PC4 and PC5 (Wilks λ = 0.987, $F_{2,173}$ =1.18, P = 0.311). In contrast, shape configurations summarized by the first three components differed between cohorts (Wilks λ = 0.325, $F_{3,172}$ = 118.82, P < 0.00001; Box M = 5.74, df = 6, P = 0.466). Separate ANOVAs controlling for FDR confirmed the role of these three components in shape differentiation (PC1: $F_{1,174}$ = 298.90, P < 0.00001; PC2: $F_{1,174}$ = 4.76, P = 0.030; PC3: $F_{1,174}$ = 7.67, P = 0.0062). Compared to 1+, 0+ trout have much lower scores for PC1 (0+ CI 95% [-0.0072, -0035]; 1+ CI 95% CI [0.0149, 0.0182]; Figure 2) and higher values for PC2 and PC3.

Allometric scaling of metabolic rate

The two age-classes differed markedly in mass (mean ± 1*SE*; age-0: 3.182 ± 0.131 g, n = 88; age-1: 9.699 ± 0.320 g, n = 88; ANOVA, $F_{1,174}$ = 474.29, P < 0.000001) and centroid size (ANOVA, $F_{1,174}$= 455.69, P < 0. 000001). In addition, the metabolic allometries differed between age-classes. Specifically, the analysis of allometric slopes revealed that the centroid size scaling exponent was higher for age-0 than for age-1 fish (ANCOVA; $F_{1,172}$ = 9.07, P = 0.0029; Figure 3; Table 1). Similarly, the mass exponent differed also between age groups ($F_{1,172}$ = 5.13, P = 0.0248; Figure 4; Table 1). The mass-scaling exponent of the older age group (b = 0.845) was 28.7% lower and outside the confidence interval of the younger age group (b = 1.185; Table 1). Finally, the observed exponent for all the fish regardless age-class (ontogenetic allometry) was very close to 1 (b = 1.036; Table 1; Figure 4).

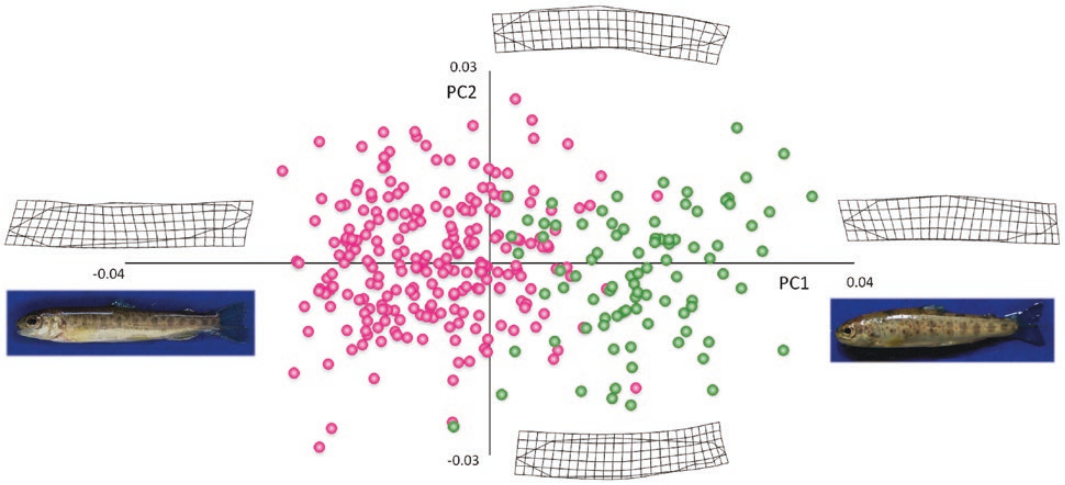

Figure 2. Scores of the PCA performed on the variances-covariances matrix for the morphological variables, and deformation grids for juvenile brown trout (0+, magenta; 1+, green). PC1 reflects a contrast between deep-bodied (higher positive scores) and elongate (higher negative scores) forms. PC2 reflects disparity in the relative position of the caudal region: high positive scores indicate a lower position of the tail. The photographs represent extreme shapes along PC1 for near-zero scores on PC2.

Ontogenetic changes in shape and metabolic rate

We conducted a multiple regression of log-SMR on PC1 (the most relevant component, associated with the elongation-robustness continuum) and log-mass or log-CS. PC1 entered the model regardless of the measure used as proxy for body size. Although most of the variation in metabolic rate is explained by the variation in body size, the degree of elongation or flatness still explains a significant amount of the variance in SMR after CS ($F_{1,173}$ = 12.11, P = 0.0006) or wet mass ($F_{1,173}$ = 4.38, P = 0.0379) entry. At the same size, robust fish showed higher metabolic rates than more elongated fish, as indicated by positive b coefficients for PC1 (Table 2). Within age groups, we verified the positive effect of PC1 on SMR in the younger age group ($F_{1,85}$ = 5.26, P = 0.0243; Table 2), confirming that more robust fish have higher metabolic rates. In contrast, after mass entered the model, the effect of PC1 on SMR was not significant within age groups (Table 2).

Discussion

Our results showed an ontogenetic change in the body shape of trout during the first year of life. Shape modifications affected mainly the elongation axis, as evidenced by a shift from relatively slender forms in young (age-0) individuals towards more robust, deep-bodied forms in older (age-1) juveniles, and were concomitant with a decrease of metabolic allometries with age (from positive alometry (b > 1) in age-0 to negative allometry (b < 1) in age-1 (Table 1, Figure 4). These results are consistent with the prediction of SA theory (decreasing b with increasing body thickness), but not with RTN theory (increasing b with increasing elongation) (Hirst et al. 2014; Glazier et al. 2015). Moreover, we found a positive covariation of shape (PC1) and metabolic rate (Table 2), with more robust fish having higher metabolic rates than more elongated fish after correcting for mass or centroid size. These results support hypothesis I, which is consistent with the pace-of-life idea, but they did not support hypothesis II regarding surface-area constraints: a larger surface area to mass ratio would imply higher maintenance costs associated to osmoregulation. Finally, the observation of metabolic isometry (b ~1), positive allometry (b > 1 for age 0+), and the decline of metabolic exponent b with age is consistent with some predictions from the surface area (SA) theory, as well as with those from other models of metabolic scaling as the resource demand (RD) or system composition (SC) theory (for a review see Glazier 2014).

We found a near-isometric ontogenetic scaling of SMR (b = 1.036; Table 1). At the within-species level, this value matches the predictions of several models of metabolic scaling, including SA, SC, RD, DEB models, and the 'metabolic-level boundaries' hypothesis (Van der Meer 2006; Glazier 2005, 2008, 2009a, b, 2010; Killen et al. 2010; Kearney and White 2012; Hirst et al. 2014). Intraspecific mass-scaling exponents for metabolic rate are often above the values predicted by the

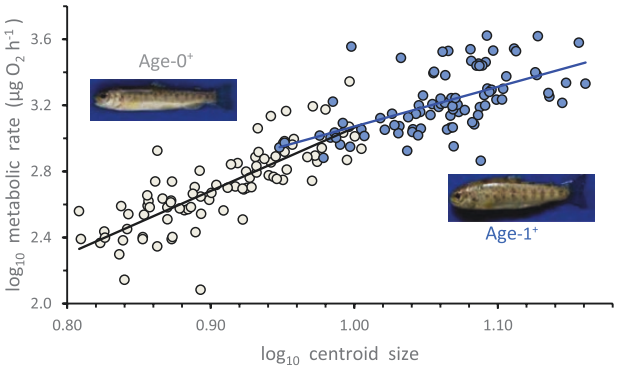

Figure 3. Metabolic allometries (standard metabolic rate on centroid size) for brown trout of ages 0+ (grey, black line) and 1+ (blue) (regression parameters: see Table 1). Logarithms were calculated on CSs and µg O_2 h^{-1} (SMR).

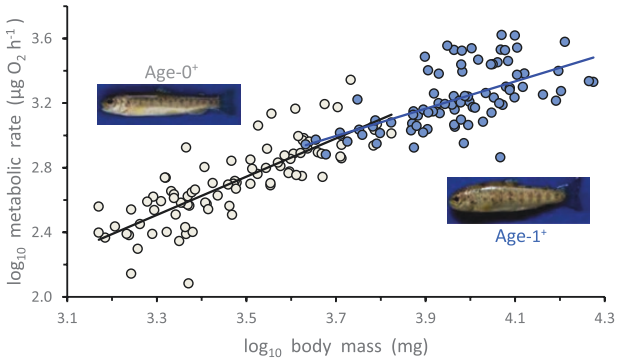

Figure 4. Metabolic allometries (standard metabolic rate on mass) for brown trout of ages 0+ (grey, black line) and 1+ (blue) (regression parameters: see Table 1). Logarithms were calculated on grams of wet mass and µg O_2 h^{-1} (SMR).

Table 1. Regression summary for allometric relationships between standard metabolic rate (log_{10} SMR) and body mass or centroid size for first- and second-year juvenile brown trout (log_{10}-transformed data)

Predictor variable	Group	*n*	$_{Adj}$-R^2	*b* [95% CI]	*SEb*	$F_{1,86}$	*P*
Body mass	Age-0	88	0.649	1.185 [1.000–1.370]	0.039	161.95	< 0.00001
(log_{10}mass)	Age-1	88	0.364	0.845 [0.610–1.081]	0.093	50.88	< 0.00001
	Total	176	0.805	1.036 [0.960–1.112]	0.032	723.02	< 0.00001
Homogeneity of slopes					$F_{1,172}$ = 5.13		0.0248
Centroid size	Age-0	88	0.637	3.830 [3.216–4.444]	0.309	153.65	< 0.00001
(log_{10}CS)	Age-1	88	0.334	2.405 [1.689–3.121]	0.360	44.59	< 0.00001
	Total	176	0.792	3.267 [3.018–3.517]	0.126	667.39	< 0.00001
Homogeneity of slopes					$F_{1,172}$ = 9.07		0.0029

Values are presented for adjusted coefficients of determination, allometric coefficients (slope, b), b confidence intervals (95%), and b standard errors. The statistical homogeneity of scaling exponents was tested by ANCOVA (slopes model).

Table 2. Results from multiple stepwise regression of metabolic rate (log_{10}-SMR) on body size (body mass or centroid size; log_{10}-transformed data) for first- and second-year juvenile brown trout

	Size predictor: log_{10} centroid size						Size predictor: log_{10} mass					
	$_{Mul}$-R^2	$_{Par}$-corr	Beta	*SE* β	t_{85}	*P*	$_{Mul}$-R^2	$_{Par}$-corr	Beta	*SE* β	t_{85}	*P*
Age 0												
Size	0.641	0.726	**0.714**	0.073	9.72	< 0.000001	0.653	0.723	**0.750**	0.078	9.66	< 0.000001
PC1	0.662	0.241	**0.168**	0.073	2.29	0.024295	0.660	0.138	0.099	0.078	1.28	0.203943
Age 1												
Size	0.341	0.592	**0.584**	0.086	6.77	<0.000001	0.372	0.605	**0.600**	0.086	7.01	< 0.000001
PC1	0.368	0.202	0.164	0.086	1.90	0.060560	0.383	0.136	0.109	0.086	1.27	0.207694
					t_{173}						t_{173}	
All												
Size	0.793	0.740	**0.752**	0.052	14.45	< 0.000001	0.806	0.746	**0.807**	0.055	14.74	< 0.000001
PC1	0.807	0.256	**0.181**	0.052	3.48	0.000635	0.811	0.157	**0.114**	0.055	2.09	0.037921

Values are presented for multiple determination coefficients ($_{Mul}$-R^2), partial correlation coefficients, standardized allometric exponent, beta (β), and the standard error for beta (*SE* β). Significant betas are shown in bold.

general RTN model (Glazier 2005, 2014; but see Van der Meer 2006; Price et al. 2007; Kearney and White 2012). The near-isometric scaling of metabolic rate has been reported for pelagic organisms (Hirst et al. 2014, 2017; Glazier et al. 2015) and fishes (Giguère et al. 1988; Post and Lee 1996). Previous fish studies suggest that the ontogenetic metabolic exponent might be in the range 0.80–0.85, but isometric or near isometric scaling for the larval stages (Giguère et al. 1988; Post and Lee 1996; Bokma 2004; Killen et al. 2007).

The ontogenetic scaling in the brown trout was nonlinear, shifting from positive to negative allometric slope between the first and second year of life (Table 1, Figure 3). The observed decline in *b* with age reinforces the evidence for nonlinearity of the ontogenetic metabolic scaling (Giguère et al. 1988; Post and Lee 1996; Glazier 2005, 2018; Moran and Wells 2007; Killen et al. 2007; Streicher et al. 2012), and suggests that the age-specific *b*-values may fall down towards a stabilizing baseline value associated with a threshold size, within the first year of life (Streicher et al. 2012). Moreover, the decrease in *b* with age may suggest a link between shape change and metabolic change, as previously shown for aquatic invertebrates (Hirst et al. 2014; Glazier et al. 2015) and young developmental stages of fishes (Giguère et al. 1988; Post and Lee 1996). Near-isometric scaling in fish larvae has been associated with steep initial scaling of gill-surface area, which would develop shallower at older ages (Post and Lee 1996; Hirst et al. 2014; Li et al. 2018), and oxygen absorption through their entire body surface. This mechanism is relevant to the present study because many larval and juvenile fish depend heavily on cutaneous respiration (Post and Lee 1996; Rombough and Moroz 1997; Glover et al. 2013; Glazier et al. 2015), and therefore would explain the link between shape shifting and change in metabolic scaling on the light of the surface-area dependence theory (Hirst et al. 2014; Glazier et al. 2015; Glazier and Paul 2017; Li et al. 2018; Scheuffele et al. 2021). In the same line, the skin of freshwater fishes is permeable to water (Talbot et al. 1982) and therefore the costs of osmoregulation are expected to change with fish size and shape (Styga et al. 2019).

In the context of system composition (SC) theory and DEB models, which incorporate principles of SC, SA and resource transport theories (Kooijman 1986, 2010; Sousa et al 2010; Kearney and White 2012; Glazier 2014), whole body mass comprises both high-energy tissues (e.g., brain, heart, or kidneys) and low-energy tissues (e.g., skeleton, muscle, and fat). Thus, body mass integrates size but also the relative proportions of different tissue types, so that it can convey differences in the ratio from nonmetabolising 'reserve' mass [which has a very low mass-corrected metabolic rate (Hsu et al. 2003; Wang et al. 2010, 2012)] to metabolising mass and overall cellular demands. This may have two main implications for the observed decline in metabolic scaling. First, we found an overdevelopment of the dorsal region in deep-bodied fish, which can correspond with a greater development of skeletal muscle over the dorsofrontal area (landmark 3; Figure 1). This is consistent with the positive coefficient of PC1 after removal of volumetric size effects on SMR, and also in agreement with both DEB (SMR proportional to structural body volume) theory (Kearney and White 2012). Second, a decline of *b* with age can be related to a change in body composition between ages 0 and 1. According to SC theory, negatively allometric scaling of metabolic rate during ontogeny can result from slow relative growth of high-energy tissues and faster relative growth of low-energy tissues (e.g., fat, skeleton and muscle) (Oikawa and Itazawa 1993, 2003; Huang et al. 2013). Since age 1 fish showed a higher muscle development than age 0 fish, and fat storage usually increase over the first years of life (e.g. Rønsholdt 1995; Deudal 2002; Hurst and Conover 2003), the difference in the metabolic exponents could be driven by lower proportions of fat and muscle tissue in the younger fish.

Finally, the ontogenetic decrease in the metabolic exponent may also indicate that metabolic scaling is affected, in addition to endogenous factors (e.g. physiology, morphology), by ecological (external) factors (Witting 1998; Killen et al. 2010; Glazier 2010, 2011, 2018, 2020a; Uyeda et al. 2017; Li et al. 2018; Hatton et al. 2019; Tan et al. 2019) and their interactions (Gjoni et al. 2020; Glazier et al. 2020b). For example, changes in resource availability, population density, or risk of predation (Biro et al. 2005) can affect growth and allocation patterns, which in turn could alter the metabolic scaling. As the costs of the growth machinery contribute strongly to metabolic rate (Rosenfeld et al. 2015) and, in teleost fish, growth

rates and mortality risk decline with age, the nonlinear, decreasing metabolic allometry can be associated with rapid growth early in ontogeny, and progressively slower growth at older ages (Glazier et al. 2011, 2020a; Tan et al. 2019; Norin 2021).

Acknowledgments

We thank Jerónimo de La Hoz, Luis Miguel Álvarez-Morales, and the staff of the Principality of Asturias for providing the experimental fish and permits to conduct the work. We wish to especially acknowledge the thoughtful work of three anonymous reviewers whose help and constructive criticisms have significantly improved the final version of the manuscript.

Funding

This work was supported by the Principality of Asturias (grant no. CN-07-164); the Spanish Government (grants no. MEC-CGL2004-03239/BOS and MMA/86-2003-1); and FICYT (predoctoral fellowship BP04-147 to J.R.S.G.)

Conflict of interest statement

We declare we have no competing interests.

Ethics

This study was conducted under permits #200450700001838 and #200660700001066 from the Government of the Principality of Asturias. Experimental protocols complied with the institutional and country legal requirements on animal welfare at the time of performing the work (RD 1201/2005) and all the procedures were conducted in accordance with the guidelines of the Research Ethics Committee of the University of Oviedo. The members of the research team have approved licenses by the Service of Animal Welfare and Production of the Principality of Asturias to conduct experimental protocols with animals (license types C and D to A.G.N). This study was carried out in compliance with the ARRIVE guidelines (Animal Research: Reporting in Vivo Experiments) for how to report animal research in scientific publications (https://arriveguidelines.org/arrive-guidelines).

Author Contributions

J.R.S.G. and A.G.N. conceived the idea and designed the experiment; J.R.S.G. reared the fish, measured metabolic rates, photographed the fish and conducted morphometric analyses; A.G.N. and J.R.S.G. performed the statistical analyses and wrote the manuscript.

Data Availability

The data supporting the results of this study are available from the Figshare Digital Repository: https://doi.org/10.6084/m9.figshare.16467531.

Supplementary Material

Supplementary data are available at *Current Zoology* online.

References

Álvarez D, Cano JM, Nicieza AG, 2006. Microgeographic variation in metabolic rate and energy storage of brown trout: countergradient selection or thermal sensitivity? *Evol Ecol* **20**: 345–363.

Álvarez D, Nicieza AG, 2005. Is metabolic rate a reliable predictor of growth and survival of brown trout *Salmo trutta* in the wild? *Can J Fish Aquat Sci* **62**: 643–649.

Archer LC, Hutton SA, Harman L, Russell Poole W, Gargan P et al., 2021. Associations between metabolic traits and growth rate in brown trout *Salmo trutta* depend on thermal regime. *Proc R Soc B* **288**: 20211509.

Arnold SJ, 1983. Morphology, performance and fitness. *Am Zool* **23**: 347–361.

Arnold PA, Delean S, Cassey P, White CR, 2021. Meta-analysis reveals that resting metabolic rate is not consistently related to fitness and performance in animals. *J Comp Physiol B* **191**: 1097–1110.

Auer SK, Anderson GJ, McKelvey S, Bassar RD, McLennan D et al., 2018b. Nutrients from salmon parents alter selection pressures on their offspring. *Ecol Lett* **21**: 287–295.

Auer SK, Dick CA, Metcalfe NB, Reznick DN, 2018a. Metabolic rate evolves rapidly and in parallel with the pace of life history. *Nat Commun* **9**: 14.

Banavar JR, Moses ME, Brown JH, Damuth J, Rinaldo A et al., 2010. A general basis for quarter-power scaling in animals. *Proc Natl Acad Sci USA* **107**: 15816–15820.

Banavar JR, Todd J, Cooke TJ, Rinaldo A, Maritan A, 2014. Form, function, and evolution of living organisms. *Proc Natl Acad Sci USA* **111**: 3332–3337.

Benjamini Y, Hochberg Y, 1995. Controlling the false discovery rate: a practical and powerful approach to multiple testing. *J R Stat Soc B* **57**: 289–300.

Biro P, Post JR, Abrahams MV, 2005. Ontogeny of energy allocation reveals selective pressure promoting risk-taking behaviour in young fish cohorts. *Proc R Soc B* **272**: 1443–1448.

Biro PA, Stamps JA, 2010. Do consistent individual differences in metabolic rate promote consistent individual differences in behavior? *Trends Ecol Evol* **25**: 653–659.

Boeuf G, Payan P, 2001. How should salinity influence fish growth? *Comp Biochem Physiol C* **130**: 411–423.

Bokma F, 2004. Evidence against universal metabolic allometry. *Funct Ecol* **18**: 184–187.

Brown JH, Gillooly JF, Allen AP, Savage VM, West GB, 2004. Toward a metabolic theory of ecology. *Ecology* **85**: 1771–1789.

Brown JH, Lasiewski RC, 1972. Metabolism of weasels: the cost of being long and thin. *Ecology* **53**: 939–943.

Burton T, Killen SS, Armstrong JD, Metcalfe NB, 2011. What causes intraspecific variation in resting metabolic rate and what are its ecological consequences? *Proc R Soc B* **278**: 3465–3473.

Cano JM, Nicieza AG, 2006. Temperature, metabolic rate, and constraints on locomotor performance in ectotherm vertebrates. *Funct Ecol* **20**: 464–470.

Careau V, Garland T, 2012. Performance, personality, and energetics: correlation, causation, and mechanism. *Physiol Biochem Zool* **85**: 543–571.

Careau V, Réale D, Humphries MM, Thomas DW, 2010. The pace of life under artificial selection: personality, energy expenditure, and longevity are correlated in domestic dogs. *Am Nat* **175**: 753–758.

Careau V, Thomas D, Pelletier F, Turki L, Landry F et al., 2011. Genetic correlation between resting metabolic rate and exploratory behaviour in deer mice *Peromyscus maniculatus*. *J Evol Biol* **24**: 2153–2163.

Claude J, 2008. *Morphometrics with R*. New York (NY): Springer.

Cutts CJ, Metcalfe NB, Taylor AC, 1998. Aggression and growth depression in juvenile Atlantic salmon: the consequences of individual variation in standard metabolic rate. *J Fish Biol* **52**: 1026–1037.

Cutts CJ, Metcalfe NB, Taylor AC, 2002. Juvenile Atlantic salmon *Salmo salar* with relatively high standard metabolic rates have small metabolic scopes. *Funct Ecol* **16**: 73–78.

Dammhahn M, Dingemanse NJ, Niemelä PT, Réale D, 2018. Pace-of-life syndromes: a framework for the adaptive integration of behaviour, physiology and life history. *Behav Ecol Sociobiol* **72**: 62.

Davies PS, 1980. Respiration in some Atlantic reef corals in relation to vertical distribution and growth form. *Biol Bull* **158**: 187–194.

Deudal M, 2002. Lipid content in rainbow trout *Oncorhynchus mykiss* fry and parr reared in spawning tributaries of Lake Taupo, New Zealand. *N Z J Mar Freshw Res* **36**: 809–814.

Djawdan M, Rose MR, Bradley TJ, 1997. Does selection for stress resistance lower metabolic rate? *Ecology* **78**: 828–837.

Dryden IL, Mardia KV, 2016. *Statistical Shape Analysis with Applications in R*. Chichester: Wiley.

Fruciano C, Tigano C, Ferrito V, 2012. Body shape variation and colour change during growth in a protogynous fish. *Environ Biol Fish* **94**: 615–622.

Giguère LA, Côté B, St-Pierre JF, 1988. Metabolic rates scale isometrically in larval fishes. *Mar Ecol Prog Ser* **50**: 13–19.

Gjoni V, Basset A, Glazier DS, 2020. Temperature and predator cues interactively affect ontogenetic metabolic scaling of aquatic amphipods. *Biol Lett* **16**: 20200267.

Glazier DS, 2005. Beyond the '3/4-power law': variation in the intra- and interspecific scaling of metabolic rate in animals. *Biol Rev* **80**: 611–662.

Glazier DS, 2008. Effects of metabolic level on the body size scaling of metabolic rate in birds and mammals. *Proc R Soc B* **22**: 405–1410.

Glazier DS, 2009a. Ontogenetic body-mass scaling of resting metabolic rate covaries with species-specific metabolic level and body size in spiders and snakes. *Comp Biochem Physiol A* **153**: 403–407.

Glazier DS, 2009b. Metabolic level and size scaling of rates of respiration and growth in unicellular organisms. *Funct Ecol* **23**: 963–968.

Glazier DS, 2010. A unifying explanation for diverse metabolic scaling in animals and plants. *Biol Rev* **85**: 111–138.

Glazier DS, 2014. Metabolic scaling in complex living systems. *Systems* **2**: 451–540.

Glazier DS, 2015. Is metabolic rate a universal 'pacemaker' for biological processes? *Biol Rev* **90**: 377–407.

Glazier DS, 2018. Rediscovering and reviving old observations and explanations of metabolic scaling in living systems. *Systems* **6**: systems6010004.

Glazier DS, Borrelli JJ, Hoffman CL, 2020a. Effects of fish predators on the mass-related energetics of a keystone freshwater crustacean. *Biology* **9**: 40.

Glazier DS, Butler EM, Lombardi SA, Deptola TJ, Reese AJ et al., 2011. Ecological effects on metabolic scaling: amphipod responses to fish predators in freshwater springs. *Ecol Monogr* **81**: 599–618.

Glazier DS, Gring JP, Holsopple JR, Gjoni V, 2020b. Temperature effects on metabolic scaling of a keystone freshwater crustacean depend on the fish-predation regime. *J Exp Biol* **223**: jeb232322.

Glazier DS, Hirst AG, Atkinson D, 2015. Shape shifting predicts ontogenetic changes in metabolic scaling in diverse aquatic invertebrates. *Proc R Soc B* **282**: 20142302.

Glazier DS, Paul DA, 2017. Ecology of ontogenetic body-mass scaling of gill surface area in a freshwater crustacean. *J Exp Biol* **220**: 2120–2127.

Glover CN, Bucking C, Wood CM, 2013. The skin of fish as a transport epithelium: a review. *J Comp Physiol B* **183**: 877–891.

Gould SJ, 1966. Allometry and size in ontogeny and phylogeny. *Biol Rev* **41**: 587–638.

Hartikainen H, Humphries S, Okamura B, 2014. Form and metabolic scaling in colonial animals. *J Exp Biol* **217**: 779–786.

Hatton IA, Dobson AP, Galbraith ED, Loreau M, 2019. Linking scaling laws across eukaryotes. *Proc Natl Acad Sci USA* **116**: 21616–21622.

Hirst AG, Glazier DS, Atkinson D, 2014. Body shape shifting during growth permits tests that distinguish between competing geometric theories of metabolic scaling. *Ecol Lett* **17**: 1274–1281.

Hirst AG, Lilley MKS, Glazier DS, Atkinson D, 2017. Ontogenetic body-mass scaling of nitrogen excretion relates to body surface area in diverse pelagic invertebrates. *Limnol Oceanogr* **62**: 311–319.

Hoffmann AA, Parsons PA, 1989. Selection for increased desiccation resistance in *Drosophila melanogaster*: additive genetic control and correlated responses for other stresses. *Genetics* **122**:837–845.

Holtby LB, Swain DP, Allan GM, 1993. Mirror-elicited agonistic behaviour and body morphology as predictors of dominance status in juvenile coho salmon *Oncorhynchus kisutch*. *Can J Fish Aquat Sci* **50**: 676–684.

Hsu A, Heshka S, Janumala I, Song MY, Horlick M et al., 2003. Larger mass of high-metabolic-rate organs does not explain higher resting energy expenditure in children. *Am J Clin Nutr* **77**: 1506–1511.

Huang Q, Zhang Y, Liu S, Wang W, Luo Y, 2013. Intraspecific scaling of the resting and maximum metabolic rates of the crucian carp *Carassius auratus*. *PLoS One* **8**: e82837.

Hurst TP, Conover DO, 2003. Seasonal and interannual variation in the allometry of energy allocation in juvenile striped bass. *Ecology* **84**: 3360–3369.

Huyghe K, Husak JF, Moore IT, Vanhooydonck B, Van Damme R et al., 2010. Effects of testosterone on morphology, performance and muscle mass in a lizard. *J Exp Zool* **313A**: 9–16.

Jackson DA, 1993. Stopping rules in principal components analysis: a comparison of heuristical and statistical approaches. *Ecology* **74**: 2204–2214.

Jarek S, 2012. mvnormtest: Normality test for multivariate variables. R package version 0.1-9. R Foundation for Statistical Computing [cited 2016 October 24]. Available from https://CRAN.R-project.org/package=mvnormtest.

Kearney MR, White CR, 2012. Testing metabolic theories. *Am Nat* **180**: 546–565.

Killen SS, Atkinson D, Glazier DS, 2010. The intraspecific scaling of metabolic rate with body mass in fishes depends on lifestyle and temperature. *Ecol Lett* **13**: 84–193.

Killen SS, Costa I, Brown JA, Gamperl AK, 2007. Little left in the tank: metabolic scaling in marine teleosts and its implications for aerobic scope. *Proc R Soc B* **274**: 431–438.

Killen SS, Glazier DS, Rezende EL, Clark TD, Atkinson D et al., 2016. Ecological influences and morphological correlates of resting and maximal metabolic rates across teleost fish species. *Am Nat* **187**: 592–606.

Kleiber M, 1947. Body size and metabolic rate. *Physiol Rev* **27**: 511–541.

Klingenberg CP, 2016. Size, shape, and form: concepts of allometry in geometric morphometrics. *Dev Genes Evol* **226**: 113–137.

Kooijman SALM, 1986. Energy budgets can explain body size relations. *J Theor Biol* **121**: 269–282.

Kooijman SALM, 2010. *Dynamic Energy Budget Theory for Metabolic Organisation*. Cambridge: Cambridge University Press.

Lagos ME, White CR, Marshall DJ, 2017. Do invasive species live faster? Mass-specific metabolic rate depends on growth form and invasion status. *Funct Ecol* **31**: 2080–2086.

Lahti K, Huuskonen H, Laurila A, Piironen J, 2002. Metabolic rate and aggressiveness between brown trout populations. *Funct Ecol* **16**: 167–174.

Lappin AK, Husak JF, 2005. Weapon performance, not size, determines mating success and potential reproductive output in the collared lizard *Crotaphytus collaris*. *Am Nat* **166**: 426–436.

Li G, Lv X, Zhou J, Shen C, Xia D et al., 2018. Are the surface areas of the gills and body involved with changing metabolic scaling with temperature? *J Exp Biol* **221**: jeb174474.

Martínez-Cotrina J, Bohórquez-Alonso ML, Molina-Borja M, 2014. Morphological and behavioural correlates of contest success in male yellow-headed geckos *Gonatodes albogularis*: sequential assessment or self-assessment? *Behaviour* **151**: 1535–1554.

Mathot KJ, Dingemanse NJ, 2015. Behaviour and energetics: unrequited needs and new directions. *Trends Ecol Evol* **30**: 199–206.

Mathot KJ, Dingemanse NJ, Nakagawa S, 2019. The covariance between metabolic rate and behaviour varies across behaviours and thermal types: meta-analytic insights. *Biol Rev* **94**: 1056–1074.

Matzkin LM, Markow TA, 2009. Transcriptional regulation of metabolism associated with the increased desiccation resistance of the cactophilic *Drosophila mojavensis*. *Genetics* **182**: 1279–1288.

McCarthy ID, 2000. Temporal repeatability of relative standard metabolic rate in juvenile Atlantic salmon and its relation to life history variation. *J Fish Biol* **57**: 224–238.
McCarthy ID, 2001. Competitive ability is related to metabolic asymmetry in juvenile rainbow trout. *J Fish Biol* **59**: 1002–1014.
McGarigal K, Cushman S, Stafford S, 2000. *Multivariate Statistics for Wildlife and Ecology Research*. New York: Springer.
McMahon T, 1973. Size and shape in biology. *Science* **179**: 1201–1204.
Metcalfe NB, Taylor AC, Thorpe JE, 1995. Metabolic rate, social status and life-history strategies in Atlantic salmon. *Anim Behav* **49**: 431–436.
Molina-Borja M, Padrón-Fumero M, Alfonso-Martín T, 1998. Morphological and behavioural traits affecting the intensity and outcome of male contests in *Gallotia galloti galloti* (family Lacertidae). *Ethology* **104**: 314–322.
Monteiro LR, 1999. Multivariate regression models and geometric morphometrics: the search for causal factors in the analysis of shape. *Syst Biol* **48**: 192–199.
Moran D, Wells RM, 2007. Ontogenetic scaling of fish metabolism in the mouse-to-elephant mass magnitude range. *Comp Biochem Physiol A Mol Integr Physiol* **148**: 611–620.
Mosimann JE, 1970. Size allometry: size and shape variables with characterizations of the lognormal and generalized gamma distributions. *J Am Stat Assoc* **65**: 930–945.
Naya DE, Bozinovic F, 2012. Metabolic scope of fish species increases with distributional range. *Evol Ecol Res* **14**: 769–777.
Nespolo RF, Sepúlveda RD, Castañeda LE, Roff DA, 2011. Effects of shape variations on the energy metabolism of the sand cricket *Gryllus firmus*: a geometric morphometric analysis. *Biol Res* **44**: 69–74.
Nicieza AG, Metcalfe NB, 1999. Costs of rapid growth: the risk of aggression is higher for fast-growing salmon. *Funct Ecol* **13**: 793–800.
Norin T, 2021. Fast ontogenetic growth drives steep evolutionary scaling of metabolic rate. *bioRxiv*. doi:10.1101/2021.03.29.437465
Norin T, Malte H, Clark TD, 2016. Differential plasticity of metabolic rate phenotypes in a tropical fish facing environmental change. *Funct Ecol* **30**: 369–378.
Oikawa S, Itazawa Y, 1993. Allometric relationship between tissue respiration and body mass in a marine teleost, porgy *Pagrus major*. *Comp Biochem Physiol A Mol Integr Physiol* **105**: 129–133.
Oikawa S, Itazawa Y, 2003. Relationship between summated tissue respiration and body size in a marine teleost, the porgy *Pagrus major*. *Fish Sci* **2003**: 69, 687–694.
Okie JG, 2013. General models for the spectra of surface area scaling strategies of cells and organisms: fractality, geometric dissimilitude, and internalization. *Am Nat* **181**: 421–439.
Peres-Neto PR, Jackson DA, Somers KM, 2005. How many principal components? Stopping rules for determining the number of non-trivial axes revisited. *Comput Stat Data Anal* **49**: 974–997.
Perry G, Levering K, Girard I, Garland T Jr, 2004. Locomotor performance and social dominance in male *Anolis cristatellus*. *Anim Behav* **67**: 37–47.
Peterson CC, Husak JF, 2006. Locomotor performance and sexual selection: individual variation in sprint speed of collared lizards *Crotaphytus collaris*. *Copeia* **2006**: 216–224.
Polverino G, Santostefano F, Díaz-Gil C, Mehner T, 2018. Ecological conditions drive pace-of-life syndromes by shaping relationships between life history, physiology and behaviour in two populations of Eastern mosquitofish. *Sci Rep* **8**: 14673.
Porter WP, Kearney M, 2009. Size, shape, and the thermal niche of endotherms. *Proc Natl Acad Sci USA* **106**: 19666–19672.
Post JR, Lee JA, 1996. Metabolic ontogeny of teleost fishes. *Can J Fish Aquat Sci* **53**: 910–923.
Price CA, Enquist BJ, Savage VM, 2007. A general model for allometric covariation in botanical form and function. *Proc Natl Acad Sci USA* **104**: 13204–13209.
Price SA, Friedman ST, Corn KA, Martinez CM, Larouche O et al., 2019. Building a body shape morphospace of teleostean fishes. *Integr Comp Biol* **59**: 716–730.
Priede IG, 1985. Metabolic scope in fishes. In: Tytler P, Calow P eds. *Fish Energetics: New Perspectives*. London: Croom Helm, 33–64.
Promislow DEL, Harvey PH, 1990. Living fast and dying young: a comparative analysis of life-history variation among mammals. *J Zool* **220**: 417–437.
R Core Team, 2019. *R: A Language and Environment for Statistical Computing. R version 3.6.1—"Action of the Toes"*. Vienna: R Foundation for Statistical Computing [cited 2019 September 01]. Available from https://www.R-project.org/.
Réale D, Garant D, Humphries MM, Bergeron P, Careau V et al., 2010. Personality and the emergence of the pace-of-life syndrome concept at the population level. *Philos Trans R Soc B* **365**: 4051–4063.
Ricklefs RE, Wikelski M, 2002. The physiology/life-history nexus. *Trends Ecol Evol* **17**: 462–468.
Rincón PA, Bastir M, Grossman GD, 2007. Form and performance: body shape and prey-capture success in four drift-feeding minnows. *Oecologia* **152**: 345–355.
Robertsen G, Armstrong JD, Nislow KH, Herfindal I, McKelvey S et al., 2014. Spatial variation in the relationship between performance and metabolic rate in wild juvenile Atlantic salmon. *J Anim Ecol* **83**: 791–799.
Rohlf FJ, 2015a. The tps series of software. *Hystrix It J Mamm* **26**: 9–12.
Rohlf FJ, 2015b. *tpsDig, Digitize Landmarks and Outlines, Version 2.22*. Stony Brook, NY: Department of Ecology and Evolution, State University of New York.
Rohlf FJ, 2016. *tpsRelw, Relative Warps Analysis, Version 1.65*. Stony Brook, NY: Department of Ecology and Evolution, State University of New York.
Rohlf FJ, Lice A, Corti M, 1996. Morphometric analysis of old world talpidae (Mammalia, Insectivora) using partial-warp scores. *Syst Biol* **45**: 344–362.
Rombough P, Moroz B, 1997. The scaling and potential importance of cutaneous and branchial surfaces in respiratory gas exchange in larval and juvenile walleye. *J Exp Biol* **200**: 2459–2468.
Rønsholdt B, 1995. Effect of size/age and feed composition on body composition and phosphorus content of rainbow trout *Oncorhynchus mykiss*. *Water Sci Thechnol* **10**: 175–183.
Rosenfeld J, Van Leeuwen T, Richards J, Allen D, 2015. Relationship between growth and standard metabolic rate: measurement artefacts and implications for habitat use and life-history adaptation in salmonids. *J Anim Ecol* **84**: 4–20.
Rubio-Gracia F, García-Berthou E, Guasch H, Zamora L, Vila-Gispert A, 2020. Size-related effects and the influence of metabolic traits and morphology on swimming performance in fish. *Curr Zool* **66**: 493–503.
Sánchez-González JR, 2015. *Morphological Disparity, Metabolic Rate, and Dispersal in Mountain Populations of Brown Trout (Salmo trutta L.)*. Thesis Dissertation. University of Oviedo.
Sánchez-González JR, Nicieza AG, 2017. Phenotypic convergence of artificially reared and wild trout is mediated by shape plasticity. *Ecol Evol* **7**: 5922–5929.
Savage VM, Allen AP, Brown JH, Gillooly JF, Herman AB et al., 2007. Scaling of number, size, and metabolic rate of cells with body size in mammals. *Proc Natl Acad Sci USA* **104**: 4718–4723.
Savage VM, Deeds EJ, Fontana W, 2008. Sizing up allometric scaling theory. *PLoS Comput Biol* **4**: e1000171.
Scheuffele H, Jutfelt F, Clark TD, 2021. Investigating the gill- oxygen limitation hypothesis in fishes: intraspecific scaling relationships of metabolic rate and gill surface area. *Conserv Physiol* **9**: coab040.
Schimpf NG, Matthews PGD, White CR, 2012. Cockroaches that exchange respiratory gases discontinuously survive food and water restriction. *Evolution* **66**: 597–604.
Sousa T, Domingos T, Poggiale JC, Kooijman SALM, 2010. Dynamic energy budget theory restores coherence in biology. *Philos Trans R Soc B* **365**: 3413–3428.
Sowersby W, Eckerström-Liedholm S, Rowinski PK, Balogh J, Eiler S et al., 2021. The relative effects of pace of life-history and habitat

characteristics on the evolution of sexual ornaments: a comparative assessment. *Evolution* **76**: 114–127.

Streicher JW, Cox CL, Birchard GF, 2012. Non-linear scaling of oxygen consumption and heart rate in a very large cockroach species *Gromphadorhina portentosa*: correlated changes with body size and temperature. *J Exp Biol* **215**: 1137–1143.

Styga JM, Pienaar J, Scott PA, Earley RL, 2019. Does body shape in *Fundulus* adapt to variation in habitat salinity? *Front Physiol* **10**: 1400.

Swain DP, Holtby LB, 1989. Differences in morphology and behavior between juvenile coho salmon *Oncorhynchus kisutch* rearing in a lake and in its tributary stream. *Can J Fish Aquat Sci* **46**: 1406–1414.

Talbot C, Eddy FB, Johnston J, 1982. Osmoregulation in salmon and sea trout alevins. *J Exp Biol* **101**: 61–70.

Tan H, Hirst AG, Glazier DS, Atkinson D, 2019. Ecological pressures and the contrasting scaling of metabolism and body shape in coexisting taxa: cephalopods versus teleost fish. *Philos Trans R Soc B* **374**: 20180543.

Uyeda JC, Pennell MW, Miller ET, Maia R, McClain CR, 2017. The evolution of energetic scaling across the vertebrate tree of life. *Am Nat* **190**: 185–199.

Valentin AE, Penin X, Chanut JP, Sévigny JM, Rohlf FJ, 2008. Arching effect on fish body shape in geometric morphometric studies. *J Fish Biol* **73**: 623–638.

Van Leeuwen TE, Rosenfeld JS, Richards JG, 2011. Adaptive trade-offs in juvenile salmonid metabolism associated with habitat partitioning between coho salmon and steelhead trout in coastal streams. *J Anim Ecol* **80**: 1012–1023.

Van der Meer J, 2006. Metabolic theories in ecology. *Trends Ecol Evol* **21**: 136–140.

Wainwright PC, 1994. Functional morphology as a tool in ecological research. In: Wainwright P, Reilly S eds. *Ecological Morphology: Integrative Organismal Biology*. Chicago: University of Chicago Press, 42–59.

Wang Z, Ying Z, Bosy-Westphal A, Zhang J, Heller M et al., 2012. Evaluation of specific metabolic rates of major organs and tissues: comparison between nonobese and obese women. *Obesity* **20**: 95–100.

Wang Z, Ying Z, Bosy-Westphal A, Zhang J, Schautz B et al., 2010. Specific metabolic rates of major organs and tissues across adulthood: evaluation by mechanistic model of resting energy expenditure. *Am J Clin Nutr* **92**: 1369–1377.

Warner RR, Schultz ET, 1992. Sexual selection and male characteristics in the bluehead wrasse *Thalassoma bifasciatum*: mating site acquisition, mating site defense, and female choice. *Evolution* **46**: 1421–1442.

West GB, Brown JH, Enquist BJ, 1997. A general model for the origin of allometric scaling laws in biology. *Science* **276**: 122–126.

West GB, Brown JH, Enquist BJ, 1999. The fourth dimension of life: fractal geometry and allometric scaling of organisms. *Science* **284**: 1677–1679.

White CR, Kearney MR, Matthews PGD, Kooijman SALM, Marshall DJ, 2011. A manipulative test of competing theories for metabolic scaling. *Am Nat* **178**: 746–754.

Witting L, 1998. Body mass allometries caused by physiological or ecological constraints? *Trends Ecol Evol* **13**: 25

Yagi S, Oikawa S, 2014. Ontogenetic phase shifts in metabolism in a flounder *Paralichthys olivaceus*. *Sci Rep* **4**: 7135.

Zelditch ML, Swiderski DL, Sheets HD, Fink WL, 2004. *Geometric Morphometrics for Biologists*. San Diego, CA: Elsevier Academic Press.